The Journal of Experimental Biology 213, 1366-1375

doi:10.1242/jeb.037945

Dynamics of optomotor responses in *Drosophila* to perturbations in optic flow

Jamie C. Theobald[1,*], Dario L. Ringach[2,3] and Mark A. Frye[1,2]

[1]Howard Hughes Medical Institute, The Department of Integrative Biology and Physiology, University of California, Los Angeles, 621 Charles Young Dr. South, Los Angeles, CA 90095-1606, USA, [2]Departments of Neurobiology and [3]Psychology, David Geffen School of Medicine, University of California, Los Angeles, Los Angeles, CA 90095-1563, USA

*Author for correspondence (jamiet@ucla.edu)

Accepted 24 December 2009

SUMMARY

For a small flying insect, correcting unplanned course perturbations is essential for navigating through the world. Visual course control relies on estimating optic flow patterns which, in flies, are encoded by interneurons of the third optic ganglion. However, the rules that translate optic flow into flight motor commands remain poorly understood. Here, we measured the temporal dynamics of optomotor responses in tethered flies to optic flow fields about three cardinal axes. For each condition, we used white noise analysis to determine the optimal linear filters linking optic flow to the sum and difference of left and right wing beat amplitudes. The estimated filters indicate that flies react very quickly to perturbations of the motion field, with pure delays in the order of ~20 ms and time-to-peak of ~100 ms. By convolution the filters also predict responses to arbitrary stimulus sequences, accounting for over half the variance in 5 of our 6 stimulus types, demonstrating the approximate linearity of the system with respect to optic flow variables. In the remaining case of yaw optic flow we improved predictability by measuring individual flies, which also allowed us to analyze the variability of optomotor responses within a population. Finally, the linear filters at least partly explain the optomotor responses to superimposed and decomposed compound flow fields.

Supplementary material available online at http://jeb.biologists.org/cgi/content/full/213/8/1366/DC1

Key words: vision, white noise, fly, optomotor response, flight control, optic flow.

INTRODUCTION

Animals use optic flow fields generated in a stationary environment to estimate self-motion (Longuet-Higgins and Prazdny, 1980), and in the aerobatic fly this is a crucial source of feedback (Egelhaaf and Borst, 1993). This bears out in evidence that the third optic ganglion in the fly visual system encodes specific patterns of optic flow (Longuet-Higgins and Prazdny, 1980; Krapp and Hengstenberg, 1996). Although a fly's visual system captures coarse images, it is extremely fast and sensitive, and ideally suited to analyze rapidly changing image motion (Autrum, 1958; Kirschfeld, 1967; Kirschfeld, 1976; Braitenberg, 1967; Hardie and Raghu, 2001).

Like gaze stabilization in humans (Miles and Wallman, 1993), a fly subjected to unplanned apparent self-motion moves to minimize the resultant optic flow across the retina. For example, in a rotating striped drum a tethered fly steers to follow the pattern (Collett, 1980a; Collett, 1980b; Mronz and Lehmann, 2008). This classical optomotor response is a central feature of a fly's flight control system, using visual motion to correct involuntary deviations from course (Poggio and Reichardt, 1976). However, animals moving through the natural world cope with compound patterns of optic flow, and for flying insects in particular the challenge is heightened by buffeting winds which in principle can elicit forces in any direction and torque around any axis.

Several models account quite well for neuronal responses and flight behavior with feedback mechanisms (Collett and Land, 1975; Götz, 1975; Poggio and Reichardt, 1976; Dickson et al., 2008). It has been shown that models that account well for these responses are insensitive to wide variations in spatial textures, but instead are largely influenced by the dynamics of naturalistic optic flow (Lindemann et al., 2005). Additionally, studies in the blowfly have revealed that linear sums of the output from HS (horizontal system) and VS (vertical system) neurons can encode translational and rotational components of self motion from naturalistic optic flow (Karmier et al., 2006). However, the dynamical behavioral responses to optic flow and the linearity of these responses have not been studied in detail. Here we describe the temporal dynamics of optomotor responses of flies to perturbations in the optic flow field. As a reference to the optic flow, we describe motion relative to three perpendicular axes aligned with the fly's body (Fig. 1A). Translational motion *along* each axis is usually referred to as lift, thrust and slip; rotational motion *around* each axis is conventionally called yaw, roll and pitch. These axes are a basis for general translation and rotation, such that superimposing them can represent arbitrarily complex motion of the fly's body.

Our approach consisted of treating the fly as a lumped control system, and measuring wing kinematics in response to visual perturbations, created by stimulating displacements through a cloud of points (see supplementary material Movie 1). The wing beat responses were then used to estimate the best linear filter (or impulse response, $h(t)$) linking changes in the optic flow field to motor control of wing kinematics. We find that the dynamics of stabilization are different for different perturbations. Additionally, despite great differences between individual measurement trials, the filters are highly predictive of the mean wing beat responses to novel random stimuli, usually accounting for half or more of the variance in stabilization responses.

MATERIALS AND METHODS

Subjects and preparation

The experimental subjects were female *Drosophila melanogaster* (Meigen) collected 4–6 days after adult eclosion. The colony was maintained on a 16 h:8 h light:dark cycle and fed on standard medium. We cold-anesthetized and tethered flies, then allowed them to recover for approximately 1 h. The dorsal thorax of each anesthetized fly was glued to a 0.1 mm diameter rigid tungsten rod which, after recovery, fixed their position in the center of the flight arena without interfering with wing beats (Fig. 1B). We used each fly for only a single experiment, with multiple conditions presented in random order. In other words, no fly saw the same pattern twice, and only rarely did two flies view patterns in the same order. The only criterion for including data in the analysis was that a fly beat its wings continuously for the duration of the test.

Stimuli and response measurements

The flight arena was a cylinder arrangement of 88×32 light emitting diodes (LEDs), which subtended 330 horizontal and 120 vertical degrees of the visual field (Duistermars et al., 2007a). The LED display was computer-controlled by serial interface with Matlab (Mathworks, Natick, MA, USA) (Reiser and Dickinson, 2008). From the vantage point of the fly individual LEDs were spaced 3.75 deg. apart, closer than their approximately 5 deg. interommatidial angles (Heisenberg and Wolf, 1984). The LEDs displayed a simulated cloud of luminous dots with a uniform random distribution (Fig. 1B), then rendered apparent movement by coherent, perspective-corrected changes in dot locations. We generated five different random dot fields each experiment day, then chose one randomly for each trial. We then animated the dots to simulate flow fields representing translations and rotations around the cardinal axes for a total of six different stimulus types (see supplementary material Movie 1 for examples). The openings in the arena at the top, bottom, and the 30 deg. strip in the rear, leave some gaps in the visual coverage, but of the 4 pi steradians in a sphere, the arena geometrically covers 9.97 steradians, or 79% of the complete visual field. The refresh rate of LED panels was of the order of MHz, well above the flicker-fusion rate for flies. Between open loop trials with the dot patterns, flies viewed a bright vertical stripe (15 deg.×120 deg. at full contrast) for 5 s, which they could fixate with closed loop feedback. This kept each fly performing active flight control between trials (Reichardt and Wenking, 1969; Heisenberg and Wolf, 1979), and reasonably ensured they entered each trial in a similar behavioral state.

During visual stimulation we tracked resultant open loop wing kinematics with an opto-electronic system that tracked two variables in real time – the difference and sum of bilateral wing beat amplitude. For the left and right wing, two time-varying voltages encoded maximum wing beat amplitude (WBA) for each stroke cycle. Offline, we then calculated the difference (left minus right amplitude, ΔWBA) and sum (left plus right amplitude, ΣWBA) for each wing beat. We used ΔWBA as a proxy for bilaterally asymmetric yaw, roll and sideslip kinematics. We used ΣWBA as a proxy for bilaterally symmetric pitch, thrust and lift kinematics.

The wing beat analyzer captures only a projection of three-dimensional wing stroke, the top down infrared shadow filtered through an optical mask, and thus could potentially sacrifice resolution, or introduce distorting effects, including nonlinearities such as saturation. But although wing kinematics are far more complex than the projections, there are several justifications for measuring the sum and difference of wing beat amplitudes. First, we carefully focus the wing traces before experiments, confirming that flies can fixate a vertical bar in closed loop, and that the responses do not saturate during normal flight. Second, ΔWBA and ΣWBA have been shown to be proportional to yaw torque and axial thrust, respectively (Götz, 1987; Frye and Dickinson, 2004; Tammero et al., 2004). Third, lift and thrust are coupled during flight (Götz and Wandel, 1984), implying ΣWBA is relevant for both. Fourth, in response to a laterally expanding flow field, flies produce roll and yaw torques of similar magnitude in addition to pure sideslip axial force (Sugiura and Dickinson, 2009). The apparent cross-talk between sideslip and yaw is evidenced by a powerful active feedback loop between ΔWBA kinematics and visual sideslip (Tammero et al., 2004). Fifth and finally, we make the assumption that ΣWBA kinematics vary systematically with pitch torque, which is not unreasonable if the optomotor stabilization of nose-up pitch and a upward lift produces ΣWBA of similar sign. Left and right wing stroke amplitudes and visual pattern position were digitized at 500 Hz and stored on a computer.

RESULTS

We began with a simple test of linearity by measuring responses to instantaneous pattern rotations (impulse functions of angular velocity). The test began when the closed loop fixation stripe disappeared and the fly viewed a static random dot pattern in open loop. Then the pattern rotated to the right at either at 1000 ms ($\delta_{t\,0}$) or 1100 ms ($\delta_{t\,100}$; Fig. 1Ci). The first condition, to characterize the impulse response, was rotation by a single pixel (3.75 degrees) at $\delta_{t\,0}$ (Fig. 1Cii). The second condition, to test time invariance, was the same rotation, but at $\delta_{t\,100}$ (Fig. 1Ciii). The third condition, to test homogeneity, was rotation at $\delta_{t\,0}$, but doubled in amplitude to two pixels (Fig. 1Civ). The fourth and final condition, to test additivity, was two serial rotations, one pixel at $\delta_{t\,0}$, and one more at $\delta_{t\,100}$ (Fig. 1Cv). In Fig. 1C, black traces show the mean ΔWBA responses, and red traces show linear predictions obtained by: shifting the first black trace by 100 ms (iii), doubling the first black trace (iv), and summing the first two black traces (v). These simple tests of time-invariance, homogeneity, and additivity represent the complete requirements of a linear time-invariant (LTI) system (Oppenheim et al., 1997). The general agreement of the black and red traces suggests that within certain limits, this formulation may approximate the translation of optic flow velocity to torque steering responses. The advantage of an LTI approximation is that the impulse response is a complete and predictive description of the system. However, a disadvantage of this measurement technique is that the traces (as in Fig. 1C) are the means of individual trials (from 364 flies), a laborious method that generates a still noisy estimate of the impulse response.

To increase efficiency and more rigorously determine the optimal linear filters, we used a variation of white noise analysis (Golomb, 1981; Ringach and Shapley, 2004) in which a binary pseudo-random sequence (a 10th order m-sequence, total 1023 values at 50 Hz) controlled the instantaneous velocity of optic flow. Cross correlating the m-sequence with the wing beat responses (after subtracting the mean and dividing by the standard deviation) produces an efficient estimate of the impulse response. Fig. 1D shows a partial m-sequence controlling yaw optic flow (i), the corresponding ΔWBA response (ii), and the resulting estimate of the impulse response (iii). In contrast to 364 flies required in Fig. 1C, this estimate required just a single trial on a single fly. At 50 Hz, the m-sequence took just over 20 s to play out. We set this rate (not to be confused with the flicker rate, which was much higher) to a value known to produce robust optomotor responses in flies (Duistermars et al., 2007a).

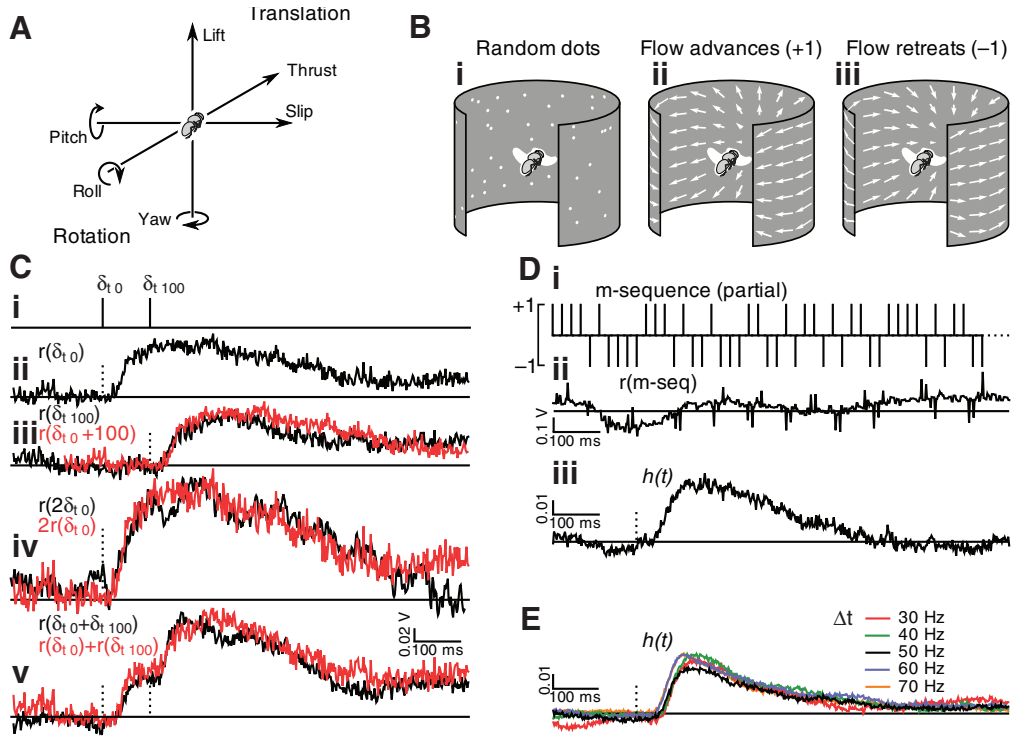

Fig. 1. The generation and modulation of optic flow fields. (A) We simulated translational and rotational motions along each cardinal axis aligned along the fly's body. (B) The stimulus was generated by simulating the perturbation of the fly's position within a cloud of randomly distributed dots (i). As the pattern advanced and retreated, the projection of dots onto a cylindrical surface was computed and the corresponding LEDs turned on (ii,iii). Arrows show the velocity of any point based on its location in the field, however, arrow lengths are approximate for the translational velocity, since 'nearer' virtual points produce faster angular speeds. (C) An impulse function modulated yaw by advancing the pattern one pixel (3.75 deg.) to the right. The top plot (i) illustrates impulses at 0 and 100 ms. (ii) The black trace below shows the difference in left and right wing beat amplitudes, the attempted turning response, to the 0 ms impulse. (iii) The response to the same increment at 100 ms, overlaid in red by the top 0 ms response shifted by 100 ms. (iv) Response to a 2 pixel increment (7.5 deg.), overlaid in red by the double top 0 ms response. (v) The response to a pattern incremented at both 0 and 100 ms, overlaid in red by the sum of the responses to 0 and 100 ms independent increments. Scale bars, 100 ms horizontally and 0.02 V vertically; each trace is the mean of responses from 364 flies. (D) The top plot (i) shows a partial m-sequence that modulated visual yaw by advancing and reversing rightward motion. (ii) The response of a single fly while viewing this yaw sequence. Scale bars, 100 ms horizontally and 0.1 V vertically. (iii) The impulse response estimated from this single fly after the full 20 s m-sequence. Scale bars, 100 ms horizontally and a correlation of 0.01 vertically. (E) Impulse response estimates obtained with m-sequences at different frame rates. The frame rate varied at 30, 40, 50, 60 and 70 Hz, and the results were averaged for 56 flies. Scale bars, 100 ms horizontally and a correlation of 0.01 vertically.

Although this parameter could influence the temporal resolution of the filter estimates, experiments indicated wide variation in frame rate had little effect (Fig. 1E, average of 56 flies).

Flight optomotor responses depend on the pattern of optic flow

Flies responded to perturbations of each of the six canonical types of optic flow and the dynamical responses to each were unique (Fig. 2, average of 68 flies). The compensating responses to translating stimuli (Fig. 2A–C) were uniformly stronger than the responses to rotating stimuli (Fig. 2D–F). Each type of optic flow with left–right symmetry (as produced by lift, thrust, and pitch) elicited strong ΣWBA modulation (Fig. 2A,B,F, column ii) but no correlated ΔWBA modulation (Fig. 2A,B,F, column i). By contrast, the flow fields containing a left–right asymmetry (as produced by yaw, slip and roll) induced substantial ΔWBA (Fig. 2C–E, column i) modulation but no correlated ΣWBA modulation (Fig. 2A,B,F, column ii). This does not necessarily mean that optic flow such as roll had no effect on ΣWBA, just that any such effect was uncorrelated with the direction of roll optic flow.

Some responses were very fast, such as for lift, thrust, slip and pitch, in which the response delay times (estimated as the time at which the signal reaches 2 standard errors above baseline) were 21, 18, 25 and 26 ms, and the times to peak response were 60, 62, 72, and 52 ms (Fig. 2Aii,Bii,Ci,Fii, green markers). These quick responses occur approximately 10 ms after the photoreceptors have begun responding to the light (Juusola and Hardie, 2001). Other responses were much slower: delay times for yaw and roll were 44 and 30 ms, and times to peak were 122 and 116 ms respectively (Fig. 2Di,Ei green markers). A third distinguishing characteristic of each response is relaxation time. The response to thrust, for example, returns to baseline (comes within two standard errors) after 389 ms (Fig. 2Bii), whereas for roll the response persists well after one second (Fig. 2Ei).

Impulse responses predict most of the explainable WBA variation

If optomotor responses are well characterized by the linear filter, then it should be possible to predict responses to a new random stimulus sequence. Therefore, we next tested whether the estimated linear filters could predict responses to novel perturbation sequences. We generated a new m-sequence and convolved it with each of the estimated impulse responses to compute predictions of wing beat responses. Then we presented randomly shifted versions of this novel

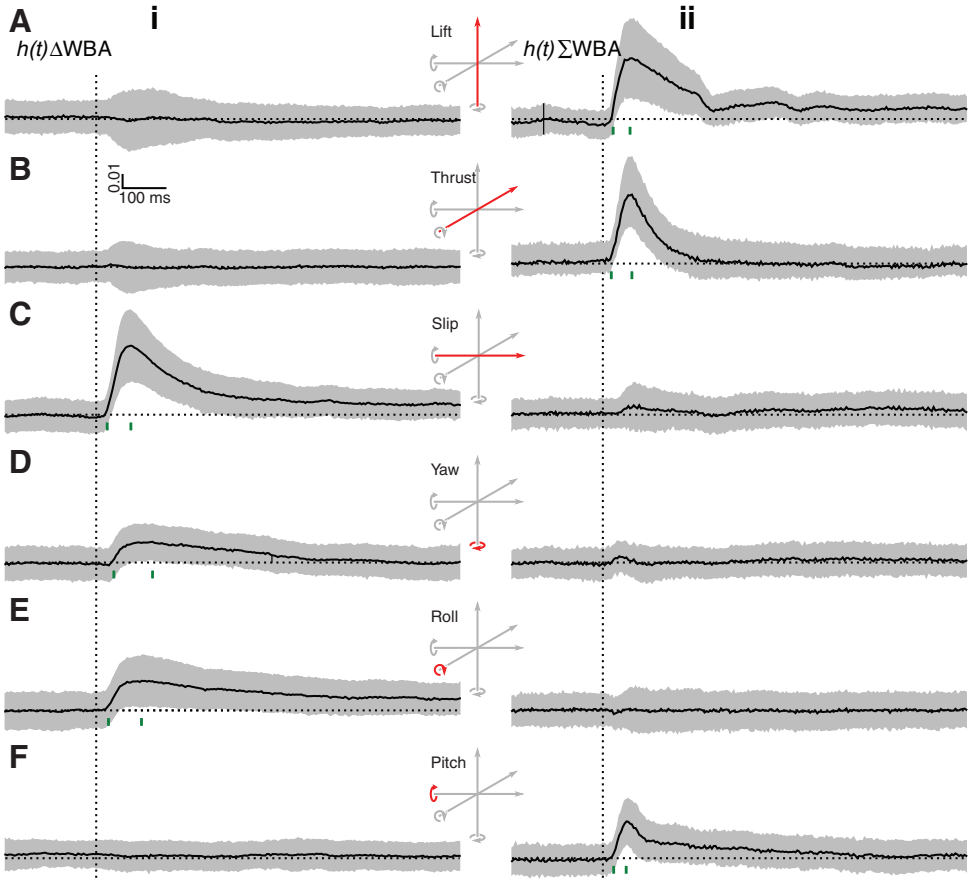

Fig. 2. Mean impulse responses to optic flow across a population of flies. The measured ΔWBA and ΣWBA impulse responses from 68 flies to each of six types of optic flow. Flies responded to left and right symmetrical stimuli, lift, thrust and pitch (A,B,F), by modulating the sum of wing stroke amplitude (ΣWBA, column ii), and asymmetrical stimuli, slip, yaw, and roll (C,D,E), by modulating the difference in wing stroke amplitude (ΔWBA, column i), relative to the velocity pattern. In each trace, the mean estimated *h(t)* is shown in black, with one standard deviation above and below it in gray. The direction considered 'positive' for each stimulus was chosen to produce a positive impulse response. The green markers below each response trace indicate the time of initial response, and the time of peak response. Scale bars, 100 ms horizontally and 0.01 units of correlation vertically.

sequence to a new group of 68 flies and averaged the temporally aligned responses. Therefore the flies and sequences used to compute the linear filters were entirely different from the flies and m-sequences used to generate comparison data. Convolving the impulse responses with each novel stimulus sequence produced the most stringent estimate possible of the deterministic component of the optomotor response.

Fig. 3A–F reproduces the responsive linear filter for each type of optic flow (Fig. 3A–Fi). The mean response to a novel 20 s m-sequence is shown in black (Fig. 3A–Fii), with one standard deviation in gray. The standard deviations of the ΣWBA responses are noticeably higher than the ΔWBA, a result of variations in focusing of wing shadows on the photodiodes. This affects the total amplitudes by shifting traces up and down, but does not reflect a less reliable metric. The dynamical model predictions, overlaid in red, are normalized to the same maximum as the black traces for graphical comparison (which does not affect the correlation coefficients). Scatter plots show the model-predicted values against measured values at each time point (Fig. 3A–Fiii, sampled at 500 Hz) of the response traces. Above this are the correlation coefficients (r), the square of which yields the coefficient of determination, or the proportion of variability accounted for by the linear filters. The correlation of all but one of the fits was above 0.7, so accounting for over half the explainable variability (the response to yaw in Fig. 3Dii was the weakest correlation and is discussed below). In the strongest case of response to sideslip, the filters accounted for over 75% (0.87^2) of the variability. Examining the scatter plots also allowed us to determine if static nonlinearities might explain even more of the variation–static because each predicted and measured pair were from the same time point, and nonlinear if we saw biases off a straight line that crossed the origin. The plots (Fig. 3iii), however, show no systematic bias away from straight lines.

As a further test of the uniqueness of the linear filters, we crosschecked each possible combination of prediction and result by calculating the coefficient of correlation. For example, do the linear filters for slip and yaw predict different wing beat responses, and might the strongly predictive slip *h(t)* better estimate yaw response than the weakly predictive yaw *h(t)*? We stress that the predicted and measured responses were generated by different flies viewing different m-sequences, so the results of this test were not a foregone conclusion. In every case, however, the strongest correlation (the best predictor of behavior) was from the correct linear filter (not shown). Surprisingly, this was true even in the case of yaw, where the linear model accounts for only about 28% (0.53^2) of the variability.

Single flies show individual impulse response variation

We were intrigued by the relatively poor predictive power of the yaw linear filter. A weak filter could be due to a noisier signal (flies may turn frequently in yaw for causes unrelated to optic flow), dynamic nonlinearities (which might be more important in the yaw plane), or because our technique of pooling the analysis over many flies masks substantial individual variability. To check for individual variability, we estimated linear filters and mean response data as above (separately collected data sets to estimate the filter and the response), but with repeated measurements on individual flies.

In order to estimate the particular *h(t)* of a single fly, we needed each animal to perform with a robust optomotor response for at least 20 min continuously while viewing repeated stimuli, as shorter times yielded noisy estimates (not shown). Because of this constraint, we

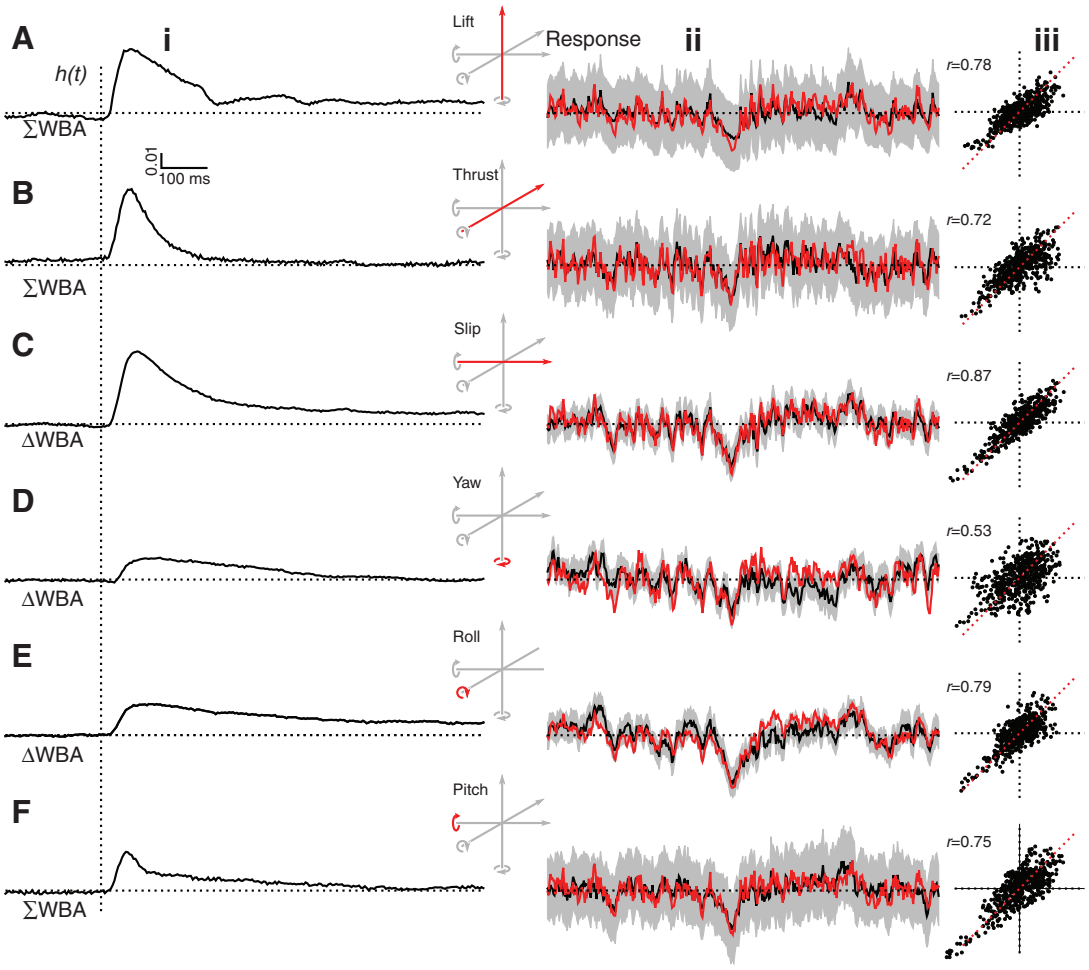

Fig. 3. Measured and predicted fly behavior. For each type of motion (A–F), the responsive linear filter, either ΔWBA or ΣWBA, appears in column i, and was used to make a prediction of the measured behavior. The mean measured responses appear in column ii in black, flanked by one standard deviation in gray. The convolution of the m-sequence and *h(t)*, the dynamical linear prediction, is traced in red. Column iii plots the predicted against observed values from corresponding time points in ii, and shows the correlation coefficient above. The scale bars by the upper left trace shows 100 ms horizontally and 0.01 units of correlation vertically. The response traces in the center are each 20 s long, and normalized to their own maximal values.

focused these experiments on the apparently weak yaw optic flow stimulus rather than testing other flow fields. We presented twenty randomly shifted m-sequences, alternated with twenty identical m-sequences, each modulating yaw optic flow. We used the randomly shifted presentations to generate estimates of individual *h(t)*, then used the repeated presentations to calculate the visually evoked variation of individual responses. As before, the sequences for generating the predictions and measuring the responses were different, although in this case, of course, the tested flies were the same.

The linear model for each of four individual flies produced a better fit than the grouped data. The individual yaw *h(t)* estimates (Fig. 4A–Di) were similar to the mean estimate, but visibly unique. As a test of similarity, we calculated the correlation coefficients of these filters to the pooled yaw *h(t)* in Fig. 2Di, and found that they ranged between 0.55 and 0.95. Consistent with this, each fly responded somewhat differently to the same m-sequence (Fig. 4A–Dii). The correlations between measured and predicted responses ranged from 0.69 to 0.85 (Fig. 4A–Diii), much higher than the 0.53 correlation based on the group estimates.

To confirm that these measured differences resulted from individual variability, not estimation error, we crosschecked linear filter predictions to responses of other flies. In this case the same flies produced the predicted and measured responses, but they were still from separate data sets collected over multiple trials. In every case again, a fly's own linear filter was the best predictor of its own response (Fig. 4E). For example, when the impulse response from the first fly was used to generate a response prediction for the second fly, the coefficient was only 0.49, rather than 0.85 obtained using the second fly's proper *h(t)*. This analysis supports the interpretation that the variation between linear filter estimates and response estimates follow directly from systematic variation in the optomotor integration of individual flies.

We tested the hypothesis that the variation between filter estimates could be explained as the superposition of a small number of components by performing a singular value decomposition (SVD) on the individual filter estimates from the four flies illustrated in Fig. 4A–D, and eight additional flies. This analysis produces a set of vectors which form a linear basis of our filters, and orders them by relative contribution [the spectrum (see Golub and Van Loan, 1996)]. In other words, we obtain a set of elementary vectors that can build any filter in our measured population by linear combination. Examining the dominant vectors can reveal whether simple components underlie a seemingly complex set of responses. The spectrum of the SVD analysis (Fig. 4Fi) shows a dominant eigenvalue, followed by one or two moderate ones. When the coefficients from the first two components of each response are plotted, there is no obvious grouping (Fig. 4Fii). Examining the shape of these two factors (Fig. 4Fiii) reveals that the first approximates a response element that is quick to peak and relaxes in about half a second (red trace), while the second approximates a response element that is slow to peak and relaxes over several seconds (blue trace). Thus, the first two components of the SVD may reflect underlying mechanisms and describe most of the variation between individual yaw filters.

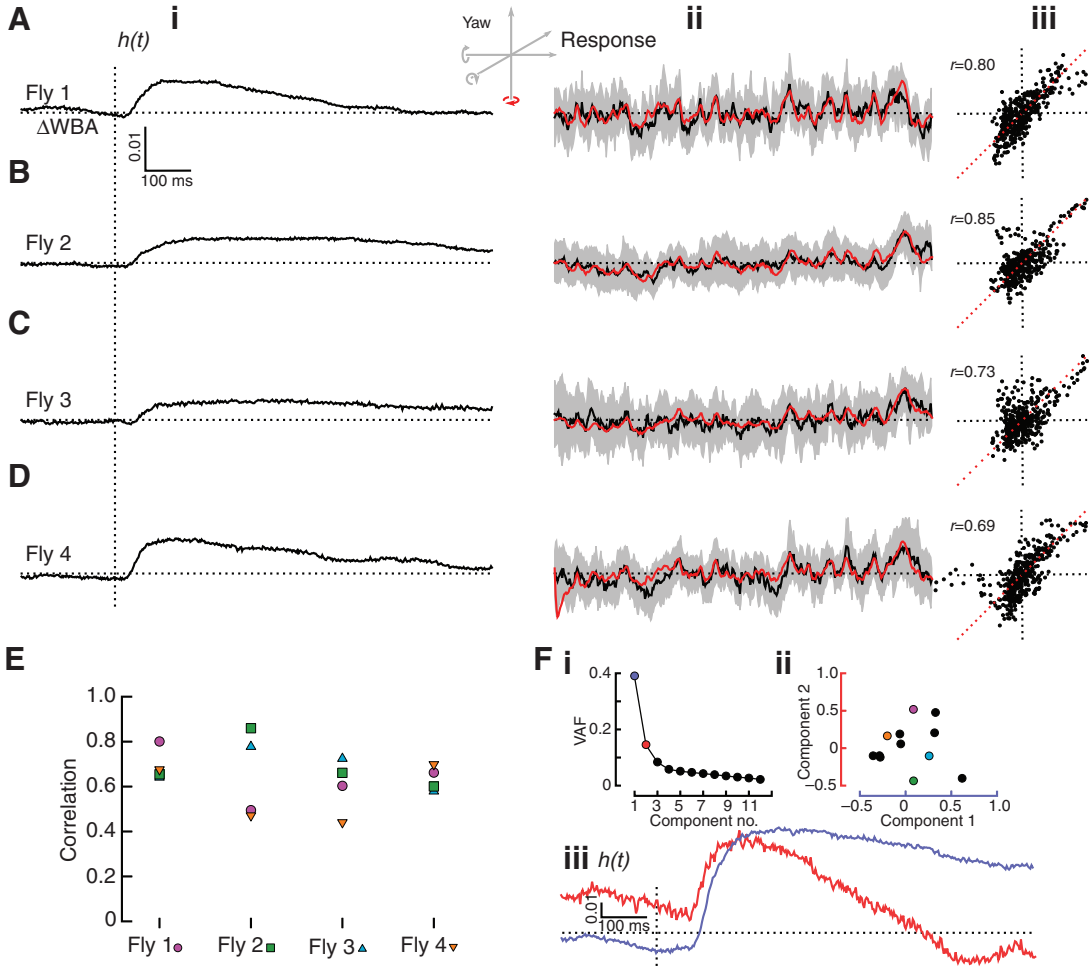

Fig. 4. Yaw *h(t)* estimates for individual flies. (A–D) Each *h(t)* in column i is the mean of twenty measurements from a single fly, produced with randomly shifted m-sequences cross correlated with the fly's ΔWBA response. Each response in column ii is the mean of twenty ΔWBA responses to aligned m-sequences, a black line flanked by one standard deviation in gray. The prediction of the linear dynamical model is superimposed on the response trace in red. Column iii plots the predicted against observed values from corresponding time points in ii, and shows the correlation coefficient above. (E) Behavioral predictions using other impulse responses of other flies produce weaker correlations. Each column represents the responses of an individual fly, and the point shapes and colors represent behavioral predictions calculated with impulse responses measured from other individuals (for example, green square is fly 2), plotted by their correlation value on the vertical axis. (F) Singular value decomposition analysis of a group of impulse responses from 12 individuals shows (i) the spectrum of the components ordered by the fraction of total variance accounted for (VAF) by each subsequent eigenvector, (ii) the family of impulse responses plotted by their first two component coefficients, and (iii) the first two principle components themselves in blue and red. The colored points in (ii) represent the individual flies from E. Scale bars, (in a and f) 100 ms horizontally and 0.01 units of correlation vertically.

Flow fields can be superimposed or decomposed

A flying insect might encounter any one of the six cardinal flow fields alone, but would more commonly experience compound optic flows, generated from simultaneous motion on multiple axes. There are 64 combinations of the basic flows and an exhaustive parameter analysis was simply beyond our means. Rather, here we focused our analysis on the effect of superimposed flow fields for a simple case that might be commonly experienced during free flight – simultaneous lift and thrust motions. From the previous experiments we knew that these motions both affect ΣWBA, and superimposed they correspond to arbitrary translation through the sagittal plane. We created a new stimulus in which two novel m-sequences modulated lift and thrust simultaneously and independently. Since the m-sequences are uncorrelated, they do not confound each other for the purpose of prediction. This produces a fairly complex stimulus, but the motion is tractable and we estimated the mean response from 75 individual flies.

We predicted the superimposed responses by convolving these sequences with the separate lift and thrust linear filters measured earlier, then adding the results. We compared the predictions to average responses of flies that viewed this compound stimulus. In at least this single case the linear model continues to provide a good fit to the data, with a correlation of 0.79 (Fig. 5). Nevertheless, static and dynamic nonlinear effects may be significant when viewing general complex flow fields and the scatter plot of predicted and observed values shows signs of static nonlinearities affecting the distribution of points (a deviation from a straight line passing through the origin).

Another question of interest was whether different parts of the motion field affect the optomotor responses. In other words, can we explain wing kinematics by the sum of responses to motion in different parts of the visual field? One difficulty is that as the size of the moving visual field is reduced, the optomotor response drops, so it becomes difficult to get a good estimate of *h(t)*. To confront this issue and

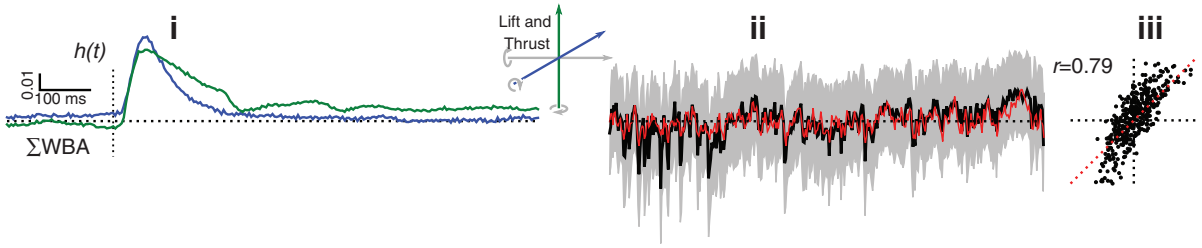

Fig. 5. Predictions for motion along two axes simultaneously. The dot stimulus simulated two orthogonal motions, lift and thrust, simultaneously modulated with different m-sequences. The kernels from Fig. 3 are reproduced here in i, and they were used to make two independent predictions of behavior. The black trace in ii shows the mean ΣWBA from 75 flies responding to the simultaneous motions, and the red trace shows the sum of the individual predictions. The scatter plot in iii shows the measured and predicted values from ii taken from simultaneous time points. Scale bars, 100 ms horizontally and 0.01 units of correlation vertically.

determine whether different parts of the visual field have unique dynamical effects on the wing beat response, we divided the visual field into right and left halves, modulated the yaw of each half-field with novel independent m-sequences, then determined the optimal linear filters linking the flow with the amplitude response of each wing.

We found that visual motion has different effects on the ipsilateral and contralateral wings (Fig. 6A, 45 flies). In response to frontward (back to front) motion in either hemisphere, both wings show impulse responses with quick peaks at 58 ms. However, the effect on the contralateral wing diminishes in just 295 ms, whereas the effect on the ipsilateral wing reverses sign after 106 ms, to become inhibitory, and remains negative for over a second. Because these are linear filters, these individual wing effects are reversed compared to patterns moving in the opposite direction. Decomposing the optic field has an additional effect of reducing the magnitude of visual responses, thus reducing the correlations to a peak of roughly 0.003.

Nevertheless, the response shapes go some way towards explaining two of the full impulse responses in Fig. 2. When both visual fields moved forward and backward together, the stimulus was similar to thrust optic flow (though not perspective-corrected). The ipsilateral and contralateral impulse responses in this case have the same sign, and, therefore, when they are added, the result is noticeably similar to the *h(t)* for thrust (Fig. 6C, black and gray traces). Likewise when each visual field moved differently, one forward and the other backward, the stimulus was yaw optic flow. In this case the impulse responses have opposite signs, and when one is therefore subtracted from the other, the result is similar to the *h(t)* for yaw (Fig. 6C, black and gray traces). Importantly, for this experiment, flies never viewed thrust or yaw stimuli (except randomly and transiently), but rather saw uncorrelated motion to the left and right. Also, since the correlations for this stimulus were much smaller, the full responses (Fig. 6B,C) were scaled down for comparison. And noticeably, the matches are imperfect, as the sum of the two in Fig. 6B has an inhibitory phase not found in the earlier thrust *h(t)* estimate, and neither Fig. 6B nor C settles with the same time course as those estimated with coordinated stimuli. This indicates the full responses are more than a linear combination of the independent ipsilateral and contralateral visual contributions to wing beat amplitude, and that nonadditive effects become important when left and right side motion are correlated.

DISCUSSION

We used a system identification approach to characterize the dynamics of optomotor responses in flies presented with simulated visual perturbations to their natural three-dimensional flight trajectories. We found that (1) flies responded to each of the six fundamental optic flow fields by modulating their wing beat kinematics with a distinctive dynamical time course (Fig. 2); (2) linear predictions from these impulse responses were often highly predictive (accounting for over half the variance) of optomotor responses, both for the population mean in every case but yaw optic flow (Fig. 3) and for individual flies in the case of the yaw (Fig. 4); (3) in some cases, responses continued to occur in a largely linear fashion even when input flow fields were superimposed (Fig. 5) or decomposed into subfields (Fig. 6).

White noise analysis has been successful for both linear and nonlinear analyses in biological systems (De Boer and Kuyper, 1968;

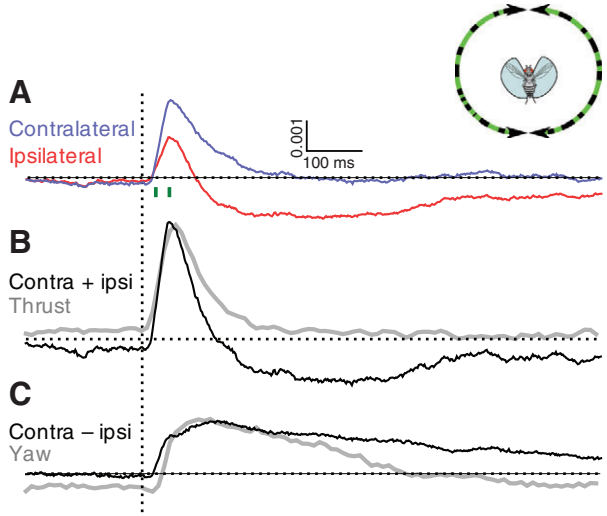

Fig. 6. Impulse responses for each wing generated from a split yaw flow field. The inset illustrates the experiment, in which random yaw patterns were modulated on the left and right with independent m-sequences. (A) The impulse responses for the ipsilateral and contralateral effect of optic flow on wing motion, estimated from 45 flies. Scale bars, 100 ms horizontally and 0.001 units of correlation vertically. (B) The sum of the ipsilateral and contralateral kernels from A, the situation expected when both hemispheres move backwards and forwards together, roughly equivalent to the thrust stimulus in the previous experiments. The thrust impulse response estimated in Fig. 3 (in gray) is shown for comparison. (C) The difference of the ipsilateral and contralateral kernels from A, expected when the fields move opposite (one forward, one backwards) and equivalent to the yaw stimulus in the other experiments. The yaw impulse response from Fig. 3 (in gray) is shown for comparison. In B and C the gray and black curves are normalized to their own maxima.

Marmarelis and Naka, 1972; Naka et al., 1979; Dickinson, 1990). It is often used to characterize responses of sensory neurons, and more rarely the behavioral output of a whole organism. But by comparison with visual processing in early motion circuits, much less is known about quantitative algorithms that transform the natural spatiotemporal patterns into the motor control of wing kinematics. However, a fundamental model supposes that insects turn in the yaw plane to equalize motion between the eyes, in other words, the inter-ocular difference in optic flow is a feedback signal to stabilize yaw (Götz, 1975; Srinivasan and Zhang, 2000; Egelhaaf and Kern, 2002). A parameterless model allowed us to measure the precise temporal dynamics of these compensating responses, and resolve even subtle differences that varied with flow fields.

Impulse response estimates for optomotor behavior

A key finding here is that each flow field produced a unique impulse response in flies, and the estimated linear filters explained up to ~75% (in the case of the sideslip flow field) of the total response variance in subsequent experiments (Fig. 3). This of course does not imply that motion *detection* (with pattern brightness as the input) is linear, as it is known to require a nonlinear interaction (Borst and Egelhaaf, 1989), rather that motion *responses* (with optic flow perturbations as the input) are linear over a substantial range of operation. Furthermore, these results do not imply linearity within the entire cascade of sensory processing and motor control, but rather that the fully integrated behavioral system is well approximated by linear filters, as over half the variance is accounted for in most cases. Within some stages, the normal operating range of the fly might mitigate underlying nonlinearities. For example, elementary motion detection shows strong nonlinearities over pattern velocity (Hausen, 1982). However, recordings from wide-field integration neurons of the lobula plate have shown that the image speeds imposing the strongest nonlinearities generally occur above those encountered during flight (Warzecha and Egelhaaf, 1996). By modulating image motion with white noise at 50 Hz such that each time step shifted the pattern in a random direction, we present multistep velocities from –188 to 188 deg. s^{-1}. It is important to keep in mind that pattern velocities outside the normal operating range of any element of the processing cascade will not evoke correlated behavioral steering responses and thus will not appear in the linear kernel estimates.

Several other aspects of our experimental method impose limitations while also providing exciting avenues for future research. Nonlinearities contained in natural scenes composed of compound patterns of flow may be asymmetrical and include motion that is independent of the fly's locomotion. It will be important to expand the present analysis to more complex optic flow regimes. Next, although the optical wingbeat analyzer takes very reliable measures in real time, it measures only a two-dimensional projection of a complicated multi-dimensional wing stroke (Fry et al., 2005). It cannot fully capture out-of-plane kinematics. Nevertheless, our results suggest that the projections themselves are consistent for a given optic flow stimulus. Our analyses were performed entirely under open-loop conditions in which the flies had no control over image motion. Closed-loop experiments with this method are more challenging but might alter the response dynamics by putting the fly in an alternative behavioral state. Finally, our experimental conditions were designed specifically to isolate optomotor responses from other important sensory inputs such as mechanosensory feedback from the halteres and odor signals from the antennae, which strongly influence the dynamics of wing-beat-mediated equilibrium responses (Sherman and Dickinson, 2004; Duistermars and Frye, 2008). During free flight these additional inputs certainly interact with the visual dynamical wing beat response.

Given these caveats, our measurements are nevertheless highly repeatable, indicating remarkable robustness in the underlying sensory-motor control algorithms. Furthermore, the potential nonlinearities imposed by the wing beat analyzer may mean our results underestimated the predictability of steering responses from linear filters. These methods and results provide a powerful analytical tool for assaying the results of genetic manipulations of underlying neural circuits.

Inter-individual variation in optomotor performance

For the yaw stimulus, our pooled estimate of the impulse response accounted for only about 28% of response variance, a poor fit by linear filters. At first glance, this low value might be expected since during sensory independent active search, flies exhibit apparently spontaneous changes in yaw (Wolf and Heisenberg, 1990; Reynolds and Frye, 2007; Chow and Frye, 2008). As repeatable as flight optomotor responses are, they show variation, and determining an underlying visual response requires averaging of multiple trials. Does this variation reflect purely random sensory-independent spontaneity or quantitative individual variation in the optomotor control system? Landing trajectories in honeybees show systematic inter-individual variation such that the angular velocity of the ground image is held constant upon approach, but the specific velocity value varies between individuals (Srinivasan et al., 1996). Flight responses in individual tethered flies are grossly similar, but show substantial differences linked to prior flight experience (Hesselberg and Lehmann, 2009).

The original experiments tested each fly only once, and it was impossible from individual trials to determine if responses between individuals varied substantially (Fig. 1D). However, when we estimated *h(t)* for individual flies by presenting a repeated yaw stimulus, we found a remarkable amount of the variation still attributable to purely linear dynamical interactions (Fig. 4A). It was a surprise to us that the correlations ranged between 0.69 and 0.85, indicating that a linear model accounts for about 49–72% of the explainable variation (as opposed to the 28% seen for the mean *h(t)* estimate), suggesting that the relatively low correlation coefficients in the population data might have resulted simply from variation between individuals. Furthermore, a fly's own unique yaw kernel produced the best prediction of its own behavioral response to a novel m-sequence (Fig. 4B). SVD analysis suggests that this variability in optomotor responses is well described by the additive contribution of a small number of underlying mechanisms (Fig. 3C). The source of this variation is unknown, but there are at least three distinct possibilities. First, there is variation in the adult phenotypes of even genetically identical animals, such as a range of masses in adult flies. The circuits that respond to yaw stimuli may exhibit this variability to a greater degree than those that respond to other stimuli. Second, flies are known to shift between different behavioral states, such as high and low activity (Rosner et al., 2009). Although the closed loop bar tracking our flies performed between trials was for the purpose of aligning their behavioral states, there are likely behavioral modes outside of those induced by recent tracking behavior. Furthermore, these could affect yaw responses disproportionately, as yaw is integral to different search strategies. Third, individual genetic differences might underlie these variations. If this is the case, the speed with which these linear estimates can be gathered on individual flies provides an entry point into analyses of the genetic and neural circuit level determinants of individual variation in optomotor performance.

Parallel subsystems for decomposing optic flow

The maximal cross-correlation between optomotor responses and the visual input stimulus was higher for translational cues than for rotational cues. This result is reminiscent of previous reports of rotational cues evoking a comparatively weak optomotor response (Duistermars et al., 2007b). An important consideration is that, although extensive, the arenas do not completely cover the flies' visual fields. Except at the poles, self rotation produces visual motion wherever there is contrast. During translation, however, visual motion also depends on object distance, and some high contrast features, such as the sun and horizon, do not appear to move. Thus the openings in the arenas may compromise the rotational simulations more than the translational ones, as these static visual areas are only plausible for translational motion.

However, the different responses may also suggest separate pathways for rotational and translational motion processing (Katsov and Clandinin, 2008). We now show two additional lines of evidence supporting this idea. First, optomotor response dynamics are strongly dependent on the perspective corrected optic-flow pattern. Second, approximate linearity extends to conditions where two types of motion field are superimposed, at least in the case of lift and thrust. Such results could most easily be attained by decomposition of the motion field into basic components, then linearly combining the responses to generate a motor command – the very method by which we generated the prediction. This is important because optic flow fields contain an enormous amount of information for an animal in nature steering its course by vision (Gibson, 1998) but only sometimes orienting to the cardinal axes, as our experiments did. Yet by showing that two superimposed translational fields moving independently generate a response that is largely the sum of each shown individually, we demonstrate a simple method for how a fly might analyze and respond to an arbitrarily complex flow field.

Individual interneurons of the third optic ganglion, which compute global features of optic flow, contain large receptive fields that locally match the retinal patterns generated during body maneuvers such as pitch and roll (Krapp and Hengstenberg, 1996; Frye and Dickinson, 2001). However, reconstructions of free flight optic flow 'played back' during electrophysiological recordings have demonstrated that individual cells respond vigorously to both translational and rotational flow fields (Kern et al., 2005). The apparent ambiguity in encoding the true instantaneous optic flow field may be computationally resolved downstream by integrating the ensemble output of cells with differing sensitivity to the compound flow fields (Karmeier et al., 2006). Whereas research on the lobula plate has provided by far the most mechanistic depth of understanding for the functional organization of optomotor behavior, there are high-order visual behaviors that cannot be easily assigned to lobula plate circuits (Theobald et al., 2008) and recently identified visual glomeruli that remain functionally unsolved (Strausfeld and Okamura, 2007). Our results complement physiological analyses of motion processing circuits by providing further quantitative evidence that optic flow fields are separately encoded and decomposed while also providing a rapid quantitative method for assessing structure–function relationships within the visual system.

The white noise analysis described here yields a precise linear dynamical profile of optomotor responses in *Drosophila*. Coupled with genetic tools, white noise analysis could help determine the role that different neural circuits contribute to the response. Both the current methods and results can be applied in a reverse-genetic screen for the putative constituent neural circuits. For example, circuit breaking techniques such as reversibly inactivating genetically targeted neural microcircuits by way of the Gal4-UAS system (Olson and Wilson, 2008) will probably uncover novel visual pathways for decomposing the retinal flow field. Further characterization of nonlinear dynamical response components could make this approach stronger still. It is important to note that the quantitative measures provided here, including the impulse responses and input–output variance functions, are not well understood at the neural circuit level. Therefore we have provided, in a genetic model organism, both a formalization of the operational algorithms and the basis by which to assay whether they are distorted.

ACKNOWLEDGEMENTS

Mark Frye is a Howard Hughes Medical Institute Early Career Scientist. This work was funded by NSF grant IOS-0718325 to M.A.F. and NIH EY-12816 and EY-18322 to D.L.R. Deposited in PMC for release after 6 months.

REFERENCES

Autrum, H. (1958). Electrophysiological analysis of the visual systems in insects. *Exp. Cell Res.* **14**, 426-439.
Borst, A. and Egelhaaf, M. (1989). Principles of visual motion detection. *Trends Neurosci.* **12**, 297-306.
Braitenberg, V. (1967). Patterns of projection in the visual system of the fly. I. Retina-lamina projections. *Exp. Brain Res.* **3**, 271-298.
Chow, D. M. and Frye, M. A. (2008). Context-dependent olfactory enhancement of optomotor flight control in *Drosophila*. *J. Exp. Biol.* **211**, 2478-2485.
Collett, T. S. (1980a). Some operating rules for the optomotor system of a hoverfly during voluntary flight. *J. Comp. Physiol. A* **138**, 271-282.
Collett, T. S. (1980b). Angular tracking and the optomotor response an analysis of visual reflex interaction in a hoverfly. *J. Comp. Physiol. A* **140**, 145-158.
Collett, T. S. and Land, M. F. (1975). Visual control of flight behaviour in the hoverfly *Syritta pipiens* L. *J. Comp. Physiol. A* **99**, 1-66.
De Boer, E. and Kuyper, P. (1968). Triggered correlation. *IEEE Trans Biomed. Eng.* **15**, 169-179.
Dickinson, M. (1990). Linear and nonlinear encoding properties of an identified mechanoreceptor on the fly wing measured with mechanical noise stimuli. *J. Exp. Biol.* **151**, 219-244.
Dickson, W. B., Straw, A. D. and Dickinson, M. H. (2008). Integrative model of *Drosophila* flight. *AIAA Journal* **46**, 2150-2164.
Duistermars, B. J. and Frye, M. A. (2008). Crossmodal visual input for odor tracking during fly flight. *Curr. Biol.* **18**, 270-275.
Duistermars, B., Reiser, M., Zhu, Y. and Frye, M. (2007a). Dynamic properties of large-field and small-field optomotor flight responses in *Drosophila*. *J. Comp. Physiol. A* **193**, 787-799.
Duistermars, B. J., Chow, D. M., Condro, M. and Frye, M. A. (2007b). The spatial, temporal and contrast properties of expansion and rotation flight optomotor responses in *Drosophila*. *J. Exp. Biol.* **210**, 3218-3227.
Egelhaaf, M. and Kern, R. (2002). Vision in flying insects. *Curr. Opin. Neurobiol.* **12**, 699-706.
Fry, S. N., Sayaman, R. and Dickinson, M. H. (2005). The aerodynamics of hovering flight in *Drosophila*. *J. Exp. Biol.* **208**, 2303-2318.
Frye, M. A. and Dickinson, M. H. (2001). Fly flight: A model for the neural control of complex behavior. *Neuron* **32**, 385-388.
Frye, M. A. and Dickinson, M. H. (2004). Motor output reflects the linear superposition of visual and olfactory inputs in *Drosophila*. *J. Exp. Biol.* **207**, 123-131.
Gibson, J. J. (1998). Visually controlled locomotion and visual orientation in animals. *Ecol. Psych.* **10**, 161-176.
Golomb, S. W. (1981). *Shift Register Sequences*. Laguna Hills: Aegean Park Press.
Golub, G. H. and Van Loan, C. F. (1996). *Matrix Computations*. Baltimore: Johns Hopkins University Press.
Götz, K. G. (1975). The optomotor equilibrium of the *Drosophila* navigation system. *J. Comp. Physiol. A* **99**, 187-210.
Götz, K. G. (1987). Course-control, metabolism and wing interference during ultralong tethered flight in *Drosophila melanogaster*. *J. Exp. Biol.* **128**, 35-46.
Götz, K. G. and Wandel, U. (1984). Optomotor control of the force of flight in *Drosophila* and *Musca* II: Covariance of lift and thrust in still air. *Biol. Cybern.* **51**, 135-139.
Hardie, R. C. and Raghu, P. (2001). Visual transduction in *Drosophila*. *Nature* **413**, 186-193.
Hausen, K. (1982). Motion sensitive interneurons in the optomotor system of the fly. *Biol. Cybern.* **46**, 67-79.
Heisenberg, M. and Wolf, R. (1979). On the fine structure of yaw torque in visual flight orientation of *Drosophila melanogaster*. *J. Comp. Physiol. A* **130**, 113-130.
Heisenberg, M. and Wolf, R. (1984). *Vision in Drosophila*. Berlin: Springer Verlag.
Hesselberg, T. and Lehmann, F. (2009). The role of experience in flight behaviour of *Drosophila*. *J. Exp. Biol.* **212**, 3377-3386.
Juusola, M. and Hardie, R. C. (2001). Light adaptation in *Drosophila* photoreceptors: I. response dynamics and signaling efficiency at 25°C. *J. Gen. Physiol.* **117**, 3-25.
Karmeier, K., van Hateren, J. H., Kern, R. and Egelhaaf, M. (2006). Encoding of naturalistic optic flow by a population of blowfly motion-sensitive neurons. *J. Neurophysiol.* **96**, 1602-1614.
Katsov, A. Y. and Clandinin, T. R. (2008). Motion processing streams in *Drosophila* are behaviorally specialized. *Neuron* **59**, 322-335.

Kern, R., van Hateren, J. H., Michaelis, C., Lindemann, J. P. and Egelhaaf, M. (2005). Function of a fly motion-sensitive neuron matches eye movements during free flight. *PLoS Biol.* **3**, e171.
Kirschfeld, K. (1967). Die projektion der optischen umwelt auf das raster der rhabdomere im komplexauge von *Musca*. *Exp. Brain Res.* **3**, 248-270.
Kirschfeld, K. (1976). The resolution of lens and compound eyes In *Neural Principles in Vision* (ed. F. Zettler, R. Weiler and D. L. Alkon), pp. 354-370. Berlin, Heidelberg: Springer Verlag.
Krapp, H. G. and Hengstenberg, R. (1996). Estimation of self-motion by optic flow processing in single visual interneurons. *Nature* **384**, 463-466.
Lindemann, J. P., Kern, R., van Hateren, J. H., Ritter, H. and Egelhaaf, M. (2005). On the computations analyzing natural optic flow: quantitative model analysis of the blowfly motion vision pathway. *J. Neurosci.* **25**, 6435-6448.
Longuet-Higgins, H. C. and Prazdny, K. (1980). The interpretation of a moving retinal image. *Proc. Roy. Soc. Lond. B.* **208**, 385-397.
Marmarelis, P. Z. and Naka, K. (1972). White-noise analysis of a neuron chain: an application of the Wiener Theory. *Science* **175**, 1276-1278.
Miles, F. A. and Wallman, J. (1993). *Visual Motion and its Role in the Stabilization of Gaze*. Amsterdam: Elsevier Science and Technology.
Mronz, M. and Lehmann, F. (2008). The free-flight response of *Drosophila* to motion of the visual environment. *J. Exp. Biol.* **211**, 2026-2045.
Naka, K. I., Chan, R. Y. and Yasui, S. (1979). Adaptation in catfish retina. *J. Neurophysiol.* **42**, 441-454.
Olsen, S. R. and Wilson, R. I. (2008). Cracking neural circuits in a tiny brain: new approaches for understanding the neural circuitry of *Drosophila*. *Trends Neurosci.* **31**, 512-520.
Oppenheim, A. V., Willsky, A. S. and Nawab, S. H. (1997). *Signals and Systems*. 2nd edn. New Jersey: Prentice Hall.
Poggio, T. and Reichardt, W. (1976). Visual control of orientation behaviour in the fly. Part II. Towards the underlying neural interactions. *Q. Rev. Biophys.* **9**, 377-438.
Reichardt, W. and Wenking, H. (1969). Optical detection and fixation of objects by fixed flying flies. *Naturwissenschaften* **56**, 424.
Reiser, M. B. and Dickinson, M. H. (2008). A modular display system for insect behavioral neuroscience. *J. Neurosci. Methods* **167**, 127-139.
Reynolds, A. M. and Frye, M. A. (2007). Free-flight odor tracking in *Drosophila* is consistent with an optimal intermittent scale-free search. *PLoS ONE* **2**, e354.
Ringach, D. and Shapley, R. (2004). Reverse correlation in neurophysiology. *Cog. Sci.* **28**, 147-166.
Rosner, R., Egelhaaf, M., Grewe, J. and Warzecha, A. K. (2009). Variability of blowfly head optomotor responses. *J. Exp. Biol.* **212**, 1170-1184.
Sherman, A. and Dickinson, M. H. (2004). Summation of visual and mechanosensory feedback in *Drosophila* flight control. *J. Exp. Biol.* **207**, 133-142.
Srinivasan, M. V. and Zhang, S.-W. (2000). Visual navigation in flying insects. *Int. Rev. Neurobiol.* **44**, 67-92.
Srinivasan, M., Zhang, S., Lehrer, M. and Collett, T. (1996). Honeybee navigation en route to the goal: visual flight control and odometry. *J. Exp. Biol.* **199**, 237-244.
Strausfeld, N. J. and Okamura, J. (2007). Visual system of calliphorid flies: Organization of optic glomeruli and their lobula complex efferents. *J. Comp. Neurol.* **500**, 166-188.
Sugiura, H. and Dickinson, M. H. (2009). The generation of forces and moments during visual-evoked steering maneuvers in flying *Drosophila*. *PLoS ONE* **4**, e4883. doi:10.1371/journal.pone.0004883.
Tammero, L. F., Frye, M. A. and Dickinson, M. H. (2004). Spatial organization of visuomotor reflexes in *Drosophila*. *J. Exp. Biol.* **207**, 113-122.
Theobald, J., Duistermars, B., Ringach, D. and Frye, M. (2008). Flies see second-order motion. *Curr. Biol.* **18**, R464-R465.
Warzecha, A. and Egelhaaf, M. (1996). Intrinsic properties of biological motion detectors prevent the optomotor control system from getting unstable. *Phil. Trans. R. Soc. Lond. B* **351**, 1579-1591.
Wolf, R. and Heisenberg, M. (1990). Visual control of straight flight in *Drosophila melanogaster*. *J. Comp. Physol. A* **167**, 269-283.